Determination of Epipolar Geometry for High Resolution Satellite Images

Myoung-Jong Noh
Department of Geoinformatic Engineering, Inha University
253 Yonghyung-dong Nam-gu, Incheon 401-751, Korea
g2031284@inhavision.inha.ac.kr

Woosug Cho
Department of Civil Engineering, Inha University
253 Yonghyung-dong Nam-gu, Incheon 401-751, Korea
wcho@inha.ac.kr

Abstract: The geometry of satellite image captured by linear pushbroom scanner is different from that of frame camera image. Since the exterior orientation parameters for satellite image will vary scan line by scan line, the epipolar geometry of satellite image differs from that of frame camera image. As we know, 2D affine orientation for the epipolar image of linear pushbroom scanners system are well-established by using the collinearity equation (Testsu Ono,1999). Also, another epipolar geometry of linear pushbroom scanner system is recently established by Habib(2002). He reported that the epipolar geometry of linear pushbroom satellite image is realized by parallel projection based on 2D affine models. Here, in this paper, we compared the Ono's method with Habib's method. In addition, we proposed a method that generates epipolar resampled images. For the experiment, IKONOS stereo images were used in generating epipolar images.

Keywords: Linear pushbroom, epipolar geometry, epipolar resampling, affine model

1. Introduction

Imagery captured from linear pushbroom scanners have been introduced for their great potential of generating ortho-photos and updating map database (Wang, 1999). The linear pushbroom scanners with up-to one-meter resolution could bring more benefits and even challenges to traditional topographic mapping with aerial images. However, the projection of satellite imagery captured with a linear scanner is quite different from that of conventional aerial photographs. This leads to failure of application of well-known epipolar geometry. Linear scanner imagery is not characterized by rigorous three dimensional perspective projection in a solid frame, but two-dimensional sequential perspective projection in a line.

To apply of epipolar geometry for linear scanner imagery, careful sensor modeling has to be adapted. Rigorous modeling describes the scene formation as it actually happens, and it has been adopted in a variety of applications (Habib, 2001; Wang, 1999; McGlone and Mikhail, 1981). Other approximate models exist such as Rational Function Model(RFM), Direct Linear Transformation(DLT), self-calibrating DLT, 2D affine orientation model, and parallel projection (Habib, 2002; Tao and Hu 2001; Dowman and Dolloff, 2000; Ono, 1999; Wang, 1999). Among these models, 2D affine orientation model (Ono, 1999) and parallel projection model (Habib, 2002) are investigated in this paper and the epipolar resampled images were generated.

2. Background

In comparison with mid resolution(5m-10m on the ground) satellite imagery such as SPOT, high-resolution (1m on the ground) satellite imagery has a much narrower field of view angle. This means that the projection of images is nearly approximated by parallel rather than central one. If conventional orientation parameters are used, very high correlation between them occurs.

The high-resolution satellite image covers a very small ground area in single scene, which is captured in a short time span on orbit. The movement of the satellite can be approximately expressed by linear or non-linear function and its attitude parameters are expected to be constant or non-constant during the short period.

1) Orun and Natarajan Model

The linear scanner at successive exposure stations has different perspective center and different attitude. Therefore, exterior orientation parameter will vary from one scan line to the others.

Kim(2000) modeled the changes of exterior orientation parameters as second order polynomial functions in scanner position and heading, and first order functions in pitch and roll angles. This model is called "Orun and Natarajan" model as cited from (Orun and Natarajan, 1994). The author proved that the epipolar line is no longer a straight line, rather has hyperbola-like shape shown in Equation (1)

$$y'=\frac{K_1 j+K_2 y+K_3}{(K_4 j+K_5 y+K_6)\sin Q(i)+(K_7 j+K_8 y+K_9)\cos Q(i)} \quad (1)$$

where j and i are the scan lines in the left and right scene, respectively. The y and y' are the point in the left and right scan line. The K_1 to K_9 are constants for a give scan line j in the left scene, and $Q(i)$ is a quadratic function of i in the right scene. In addition, the author proved that epipolar lines do not exist in conjugate pairs.

2) Straight-Line Constant-Speed Trajectory Model

This model represents the changes of exterior orientation parameters as first order polynomial functions in scanner position and constants in scanner attitudes. Hence, such a representation of exterior orientation parameters is generating images that captured in straight-line constant-speed trajectory conditions. This model was adopted by both Ono and Habib.

3) Parallel Projection Model(Habib, 2002)

The motivations for selecting the parallel projection model to approximate the rigorous model are as follows:

- Many space scanners have narrow AFOV – e.g., it is less than 1° for IKONOS scenes. For narrow AFOV, the perspective light rays become closer to being parallel.
- Space scenes are acquired within short time - e.g., it is about one second for IKONOS scenes. Therefore, scanners can be assumed to have same attitude during scene capturing. As a result, the planes, containing the images and their perspective centers, are parallel to each other.
- For scenes captured in very short time, scanners can be assumed to move with constant velocity. In this case, the scanner travels equal distances in equal time intervals. As a result, same object distances are mapped into equal scene distances.

Therefore, many space scenes, such as IKONOS, can be assumed to comply with parallel projection.

3. Approximate geometric model for linear scanner imagery

1) 2D Affine Orientation Model

Linear scanner image is captured by one-dimensional central perspective and each scan line has different exterior orientation. Also, the scene is projected to the image by parallel projection and the focal length can be set to infinity. In accordance with straight-line constant-speed trajectory model, the collinearity equation for linear scanner image can be represented in Equation (2).

$$\begin{aligned} 0 &= m_{11}(X - X_{0i}) + m_{12}(Y - Y_{0i}) + m_{13}(Z - Z_{0i}) \\ y &= m_{21}(X - X_{0i}) + m_{22}(Y - Y_{0i}) + m_{23}(Z - Z_{0i}) \end{aligned} \quad (2)$$

where m_{ij} ($i=1,2$; $j=1,2,3$) are elements of the rotation matrix between the object and scene coordinate system.

Line number i is expressed by Equation (3) using exterior orientation parameters and collinerity equations.

$$i = \frac{m_{11}(X - X_0) + m_{12}(Y - Y_0) + m_{13}(Z - Z_0)}{m_{11}\Delta X + m_{12}\Delta Y + m_{13}\Delta Z} \quad (3)$$

Now, line number i can be replaced by image coordinate x. Equation (4) arranged for the constant coefficients is described by algebraic expression.

$$\begin{aligned} x &= A_1X + A_2Y + A_3Z + A_4 \\ y &= A_5X + A_6Y + A_7Z + A_8 \end{aligned} \quad (4)$$

where A_i ($i=1,\ldots,8$) are indepentent coefficients which are called "2D Affine Orientation Parameters". Equation (4) describes the collinearity relationship between the coordinates (x,y) and the ground coordinates (X,Y,Z).

2) Parallel Projection Model

Figure 1 depicts a scene captured according to parallel projection.

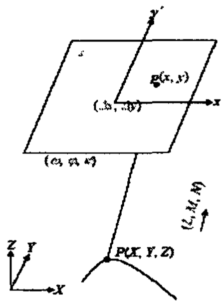

Fig. 1. Parallel projection parameters

Scene parallel projection parameters include: two components of the unit projection vector (L,M); orientation angles of the scene (ω,φ,κ); two shift values $(\Delta x,\Delta y)$; and scale factor (s). Utilizing these parameters, the relationship between an object space point $P(X,Y,Z)$ and the corresponding scene point $p(x,y)$ can be expressed in Equation (5).

$$\begin{pmatrix} x \\ y \\ 0 \end{pmatrix} = s\lambda R^T \begin{pmatrix} L \\ M \\ N \end{pmatrix} + s.R^T \begin{pmatrix} X \\ Y \\ Z \end{pmatrix} + \begin{pmatrix} \Delta x \\ \Delta y \\ 0 \end{pmatrix} \quad (5)$$

where R is the rotation matrix between the object and scene coordinate system, N is the Z-component of the unit projection vector, λ is the distance between the object and image points, which can be computed the third equation in (5).

Using sraight-line constant-speed trajectory model and 2D affine orientation model, equation (5) can be reduced to a linear form in Equation (6).

$$\begin{aligned} x &= A_1X + A_2Y + A_3Z + A_4 \\ y &= A_5X + A_6Y + A_7Z + A_8 \end{aligned} \quad (6)$$

where A_i ($i=1,...,8$) are called linear parallel projection parameters.

It is important to mention that 2D Affine Orientaiton Parameter are not related to six exterior orientation parameters, but linear parallel projection parameters are related to nine scene parallel projection parameters. Therefore, if GCPs are available, nine scene parallel projection parameters can be retrieved by utilizing the linear parallel projection parameters (Habib, 2002).

4. Approximate Epipolar Geometry of linear scanner image

1) Image Transformation

In reality, original scenes captured by linear scanner are taken central-perspectively along the scan line. For rigorous analysis, scene transformation needs to apply the parallel projection geometry.

Such a transformation alters the scene coordinates along the scan lines to make them conform to the parallel projection (Habib, 2002; Ono, 1999).

$$y = y_{ori} / (1 - (\tan\omega) y_{ori} / c)) \qquad (7)$$

where c is the scanner principal distance, ω is the scanner roll angle, y_{ori} is the coordinates along the scan line of original scene, y is the coordinates along the scan line according to parallel projection.

1) Epipolar Resampling

First, the direction of the epipolar line must be determined. The epipolar line equation can be expressed as Equation (8) (Habib, 2002; Ono, 1999).

$$G_1 x_l + G_2 y_l + G_3 x_r + G_4 y_r = 1 \qquad (8)$$

From Equation (8), it can be easily seen that epipolar lines are straight in the parallel projection. Using known corresponding points more than 4 between left and right scene, independent coefficients G_i can be determined. To generate the nomalized image, rotation angle, scale and shift of each scene must be applied to obtain corresponding epipolar lines along the same row. Such a transformation can be expressed as Equation (9).

$$\begin{pmatrix} x_n \\ y_n \end{pmatrix} = \begin{pmatrix} \cos\theta & \sin\theta \\ -\sin\theta & \cos\theta \end{pmatrix} \begin{pmatrix} x \\ y \end{pmatrix}$$
$$\begin{pmatrix} x'_n \\ y'_n \end{pmatrix} = S \begin{pmatrix} \cos\theta' & \sin\theta' \\ -\sin\theta' & \cos\theta' \end{pmatrix} \begin{pmatrix} x' \\ y' \end{pmatrix} + \begin{pmatrix} 0 \\ \Delta y \end{pmatrix} \qquad (9)$$

where θ is the rotation angle of the left scene, θ' is the rotation angle of the right scene, S is the scale factor of the right scene, and Δy is the y shift of the right scene, (x_n, y_n) and (x'_n, y'_n) are the coordinates in the left and right scene after transformation.

These transformation parameters are related to independent coefficients G_i such as followed equation (10).

$$\theta = \arctan(-G_1 / G_2),\ \theta' = \arctan(-G_3 / G_4)$$
$$\Delta y = -\frac{\sin\theta}{G_1} = \frac{\cos\theta}{G_2},\ S = \frac{G_3 \Delta y}{\sin\theta'} = -\frac{G_4 \Delta y}{\cos\theta'} \qquad (10)$$

Then, the linear scanner scenes after transformation can be considered as affine images (Ono, 1999). Therefore, the left scene and right scene are transformed by 2D affine transformation.

Let the virtual plane be a plane parallel to the right scene. The relationship between the left scene point coordinates (x_l, y_l) and the corresponding right scene point coordinates (x_r, y_r) is simply described in the following form:

$$x_l = K_1 x_r + K_2 y_r + K_3$$
$$y_l = K_4 x_r + K_5 y_r + K_6 \qquad (11)$$

where K_i ($i=1,...,6$) are independent coefficients (i.e. 2D affine parameters). Because number of unknown parameters is 6, the equation (11) can be solved if more than 3 known points are given.

Utilizing 2D affine parameters, left scene are transformed to the virtural plane. Finally, the epipolar resampled image (i.e. nomalized image) can be generated using several resampling methods.

5. Experiments

For a study of epipolar resampling, a panchromatic stereopair of IKONOS scenes covering Daejeon is used in the experiment. Data information of these scenes is shown in Table1.

Table 1. Data information of IKONOS scenes.

IKONOS	Forward scene	Backward scene
Acquisition date	2001.11.19.	2001.11.19.
Preprocessing Level	Radiometrically corrected	Radiometrically corrected
Acqusition height	681km	681km
Focal length	10m	10m
Bits per Pixel	11bits	11bits
Spatial Resolution	1m	1m

An overview of these scenes is shown in Fig. 2. An overview of 12 tie-points distribution is shown in Fig.3. The developed approach of epipolar resampling was generated by only tie-points in the experiment. The Table 2 indicates the y-parallax between left and right epipolar line using tie (12 points in total) and check-points (12 points in total). From Table 2, maximum value of y-parallax is 1.586 pixel, minimum one is 0.414 pixel, and the root mean square error is 1.079 pixel about tie-points.

About check-points, maximum value of y-parallax is 2.501 pixel, minimum one is 0.281 pixel, and the root mean square error is 1.489 pixel. As result, generated epipolar resampled images exist y-parallax insignificantly.

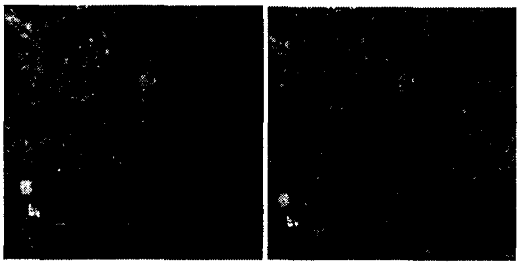

Forward scene Backward scene

Fig. 2. Overview of the IKONOS scenes.

Fig. 3. Overview of tie and check-points distribution.

Table 2. Y-parallax between left and right epipolar line.

ID	1	2	3	5	8	9	10
Tie point	0.788	-0.630	-1.586	1.575	1.347	-0.909	0.414
ID	12	17	18	19	21	RMSE	
	-0.885	1.111	0.579	-0.816	-0.989	+/- 1.079	
ID	22	23	24	28	31	36	38
Check point	0.665	-2.202	1.084	-2.433	2.501	1.891	0.851
ID	39	40	43	44	46	RMSE	
	1.192	-1.754	-1.075	1.494	0.281	+/- 1.489	

6. Conclusions

In this paper, existing two methods to generate epipolar resampled image are utilized. A modified approximate epipolar geometry are generated by combining two methods. The advantage of this geometry is that it can be used to generate indirectly epipolar reasmpled image using only tie-point. Experimental results using IKONOS data showed the feasibility of the epipolar resampling procedure.

Future work will investigate different models that are more rigorous than developed model. In addition, feasibility of the RFM model will be researched for generating the epipolar geometry.

Acknowledgement

This research was supported by University IT Research Center Project.

References

[1] Cho, W., T. Schenk, and M. Madani, 1992. Resampling Digital Imagery to Epipolar Geometry, *IAPRS International Archives of Photogrammetry and Remote Sensing*, 29(B3): 404-408.

[2] Dowman, I., and J. Dolloff, 2000. An Evaluation of Rational Functions for Photogrammetric Restitutions, *International Archives of Photogrammetry and Remote Sensing*, 33(Part B3): 254-266.

[3] Habib, A., M. Morgan, K. Kim, and S. Jeong, 2004. Parallel projection modeling for linear array scanner scenes, *International Society of Photogrammetry and Remote Sensing 12-23 July(CD-ROM)*, Istanbul.

[4] Habib. A, M. Morgan, K. Kim, and S. Jeong, 2004. Indirect epipolar resampling of scenes using parallel projection modeling of linear array scanners, *International Society of Photogrammetry and Remote Sensing 12-23 July(CD-ROM)*, Istanbul.

[5] Kim, T., 2000. A study on the epipolarity of linear pushbroom images, *journal of Photogrammetric Engineering & Remote Sensing*, 66(8):961-966

[6] Ono, T., Y. Honmachi, and S. Ku, 1999. Epipolar resampling of high resolution satellite Imagery, *Joint Workshop of ISPRS WG I/1, I/3 and IV/4 Sensors and Mapping from Space.*

[7] Orun, A., and K. Natarajan, 1994. A Modified Bundle Adjustment Software for SPOT Imagery and Photography: Tradeoff, *Journal of Photogrammetric Engineering & Remote Sensing*, 60(12): 1431-1437

[8] Tao, V. and Y. Hu, 2001. A Comprehensive Study for Rational Function Model for Photogrammetric Processing, *Journal of Photogrammetric Engineering & Remote Sensing*, 67(12):1437-1357